Single-Walled Carbon Nanotubes and C₆₀ Encapsulated by a Molecular Macrocycle

Jwa-Min Nam,* Mark A. Ratner,* Xiaogang Liu, and Chad A. Mirkin

Department of Chemistry and Institute for Nanotechnology, Northwestern University, 2145 Sheridan Road, Evanston, Illinois 60208-3113

Computational simulations of macrocycle-encapsulated single-walled carbon nanotubes (SWNTs) and C_{60} are reported. A molecular mechanical force field method has been used to calculate the physical properties of these complexes. The calculation shows that the macrocycle-encapsulated SWNTs and C_{60} are more stable than free SWNTs and C_{60}. When macrocycles are bound to SWNTs, energetically stable well regions have been observed. The energetic and dipolar changes of an armchair SWNT upon binding by a macrocycle are different from those of a zigzag SWNT. SWNTs with pentagon−heptagon defects are compared with normal SWNTs. Calculated large energetic stabilization in a water environment suggests that wrapping inorganic macrocycles around SWNTs can promote the solubility of SWNTs.

Introduction

Discovery of nanoscale carbon materials such as carbon nanotubes and buckyballs (C_{60}) has led to extensive studies of their chemical, electrical, and mechanical properties.[1−6] The relationships among physicochemical properties, the orientation of the six-membered carbon rings, and the type and size of the single-walled carbon nanotubes (SWNTs) have been of special interest.[7] SWNTs show intriguing properties due to their unique structural architectures. The diameter and helicity of SWNT can be characterized by the vector, $\mathbf{c}_h = n\mathbf{a}_1 + m\mathbf{a}_2$ ($\mathbf{a}_1$ and $\mathbf{a}_2$ are the graphene lattice vectors, and n and m are integers). Zigzag SWNTs are either metals (if $n/3$ is an integer) or semiconductors (if $n/3$ is not an integer), while armchair SWNTs are metallic when isolated.[8] Moreover, SWNTs are extremely stiff and also elastic against environmental stress.[9,10] Tuning the physical properties of SWNTs will be useful for the applications of SWNTs to electronics. The sticky nature of SWNTs has been a critical problem in controlling SWNTs. It will be impossible to control the physical properties and to fabricate SWNTs without commanding aggregation properties of SWNTs. However, it has been very difficult to control the chemical and physical properties of SWNTs.

Chemical functionalization such as defect-group functionalization, covalent sidewall functionalization, noncovalent exohedral functionalization with surfactants and polymers, and endohedral functionalization is an attractive way to improve solubility and processibility and allow the unique properties of SWNTs to be coupled to those of other types of materials.[11] The noncovalent functionalization of SWNTs can manipulate the electrical, mechanical, and aggregating properties of SWNTs without disrupting the bonding network of the nanotubes, and there have been several studies both computational and experimental concerning interactions between SWNTs and polymers for altering the physicochemical properties of polymers and SWNTs.[12,13] This polymer wrapping also increases the solubility of SWNTs in water.[14] Recently, a 1D array of C_{60} molecules nested inside an SWNT has been reported and energetics studies

have appeared.[15−17] It was indicated that insertion of C_{60} into an SWNT can be an exothermic process, and that such modification of an SWNT by intermolecular interaction can alter the physical properties of the SWNT. Most recently, electronic measurements of C_{60}@SWNT with a scanning tunneling microscope have been made showing that C_{60}@SWNT modified the local electronic structure of the nanotube.[17]

In this paper, we focus on encapsulation of C_{60} and SWNT by metallomacrocyclic rings. A novel tetranuclear rhodium complex has been synthesized from flexible hemilabile ligands, *N,N'*-dimethyl-*N,N'*-bis[2-(diphenylphosphino)ethyl]-1,4-phenylenediamine, and a "Rh(I) source" via the "weak-link synthetic approach".[18] Significantly, the complex can be reacted with small molecules (e.g., CO, $(CH_3)_4NCl$, CH_3CN, etc.) that selectively break the N−Rh links to afford flexible, 52-membered tetranuclear macrocycles, Figure 1.[18] These macrocycles are unique because of their sizes, the choice of the redox-active group, and the presence of the coordinatively unsaturated rhodium(I) metal centers in the macrocyclic framework. The macrocycles feature large cavities with electron-rich *N,N,N'N'*-tetraalkyl-1,4-phenylenediamine groups in the macrocyclic framework, which can be a significant driving force for the encapsulation of electron-deficient molecules (e.g., SWNTs and C_{60}). Numerous accounts of metal-coordinated C_{60} complexes have been reported, in which all the metals are bound in an η^2-fashion.[19−22] It can be anticipated that these flexible macrocycles might promote significant interactions between the Rh metal centers and the encapsulated SWNTs and C_{60}, and furthermore change their chemical and physical properties. More significantly, varying the coordination environment around the rhodium center with small ligands such as CH_3CN and Cl (Figure 1) can alter the interactions between the macrocycle and target molecules such as SWNTs. While internanotube interactions can be weakly altered by C_{60} insertion, encapsulating SWNTs from the outside is more effective, with more choices for controlling intermolecular interactions between SWNTs. Consequently, encapsulating SWNTs with proper macrocycles can be a way to modify the properties of a given SWNT and to control the aggregation properties of SWNTs. In this research, computer simulations of noncovalent modifications arising from

* To whom correspondence should be addressed. Fax: (+1) 847-467-5123. E-mail: ratner@chem.nwu.edu (M.A.R.); j-nam@northwestern.edu (J.-M.N.).
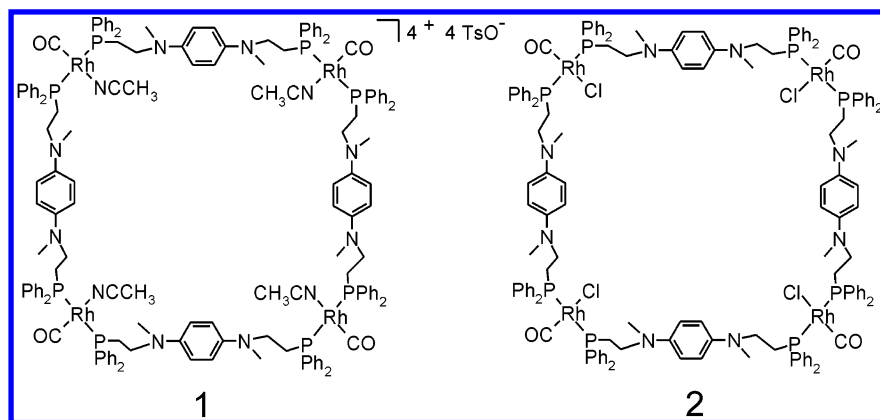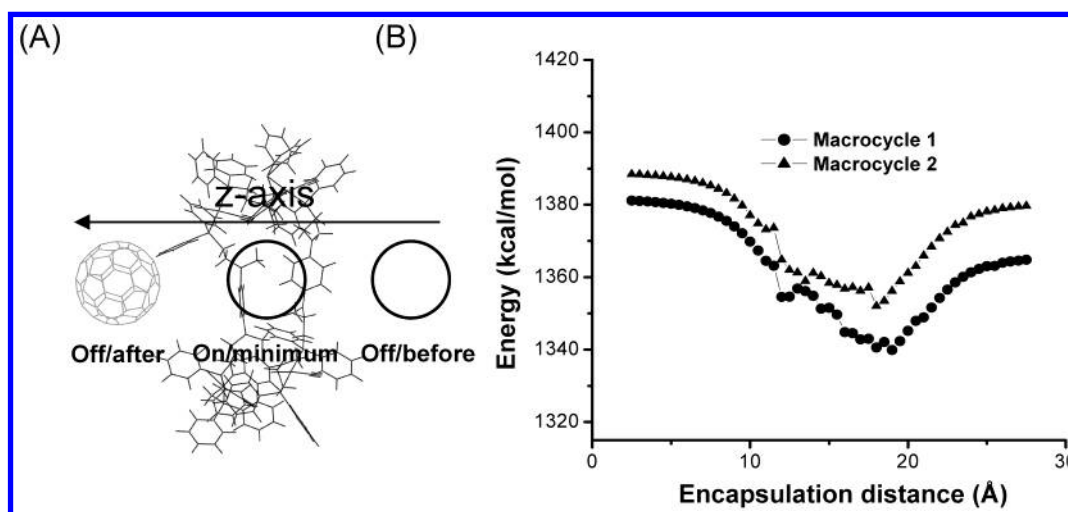
Figure 1. Inorganic macrocycles.

Figure 2. C_{60} stabilization by macrocycle encapsulation. (A) Encapsulation direction for the C_{60}/macrocycle complex. (B) Energetic profile of the C_{60}/macrocycle complex.

encapsulation of an SWNT and C_{60} by inorganic macrocycles are discussed. The desolvation energy problem for the complete encapsulation of a nanotube with an inorganic macrocycle are also discussed.

Computational Details

An MM+ force field method[23−25] has been used to optimize molecular structures and calculate the energies of the molecular systems in this research. A conjugate gradient (Polak−Ribiere) method with bond dipoles and no cutoff options has been applied for the geometric optimization of the molecular structures. Macrocycles (Figure 1) and SWNTs were optimized individually until the root-mean-square (RMS) gradient was less than 0.2 kcal/(Å mol) and C_{60} was minimized until the RMS gradient was less than 0.1 kcal/(Å mol) before encapsulation simulation. To maintain a square planar structure for the rhodium coordination sphere, 1000 kcal/mol·$Å^2$ was taken as the force constant for the spring (harmonic oscillator) between rhodium and coordinated atoms during optimization, and these constraints were removed for the single-point energy calculations of the optimized structures. For C_{60} encapsulation, optimized geometries and energies have been calculated for every 0.5 Å movement along the z-axis (Figure 2A). For the nanotube encapsulation, armchair (8, 8) and zigzag (14, 0) nanotubes with dimensions $12 \times 12 \times 41$ $Å^3$ were used. Macrocycle **1** has been used for SWNT encapsulation and moved in increments of 1 Å from one edge of the nanotube to the other with full geometric optimization at each step (Figure 3). For the desolvation energy

calculations for the nanotube, an explicit water model (TIP3P) with the switched-cutoff option has been used.[26] RMS gradient termination conditions of the optimizations for C_{60}, SWNTs, and solvated SWNTs are 0.2, 0.3, and 0.3 kcal/(Å mol), respectively.

Results and Discussion

C_{60}. The MM+-optimized energies of macrocycles **1** and **2** are 1114.1 and 1121.3 kcal/mol, respectively, and the total energy of the minimized C_{60} is 267.6 kcal/mol. Upon complexation of C_{60} by both macrocycles, there is clear energetic stabilization (Figure 2B). From the net difference between the energy before contact and the minimized energy after complexation, we can evaluate the encapsulation stabilization energy (E_{encap}). E_{encap} is defined as

$$E_{encap} = E_{on/minimum}(C_{60}/\text{macrocycle complex}) - (E_{off/before}(C_{60}) + E_{off/before}(\text{macrocycle}))$$

E_{encap} for macrocycle **1** is −41.3 kcal/mol, and E_{encap} for macrocycle **2** is −36.4 kcal/mol. Energetically, macrocycle **1** is slightly more favored for the encapsulation of C_{60}. This demonstrates that ligand substitutions on the macrocycles can produce different energetic stabilities of these complexes. For both macrocycles, there are no energetic barriers to overcome for the complete encapsulation and C_{60} prefers to stay bound to the macrocycle. In the process of disengagement of an inorganic macrocycle from C_{60}, however, there are the energetic
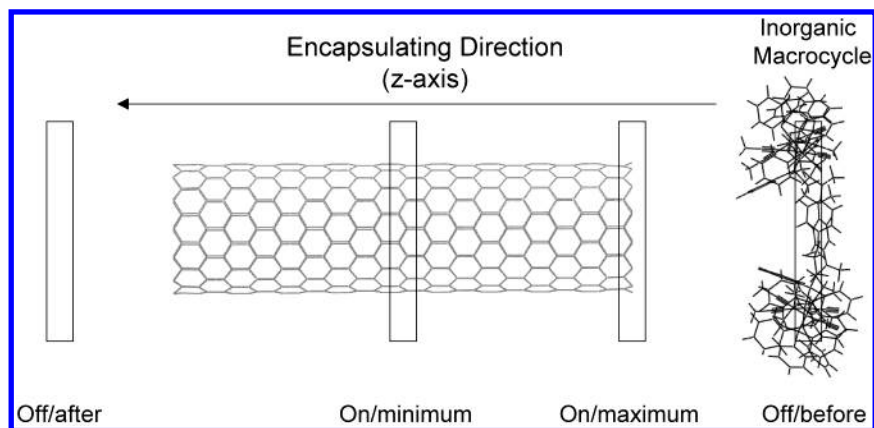
SWNTs and C$_{60}$ Encapsulated by a Macrocycle

J. Phys. Chem. B, Vol. 107, No. 20, 2003 **4707**

Figure 3. Macrocycle encapsulation onto SWNTs.

TABLE 1: Correlation Coefficients (R) with Total Energy^a

	E_{bond}	E_{angle}	E_{dih}	E_{vdW}	$E_{str-bend}$	E_{ele}
			(A) C$_{60}$			
$R_{cycle\ 1}$	0.22	0.84	0.67	0.95	0.66	−0.38
$R_{cycle\ 2}$	0.43	0.74	0.65	0.95	0.41	−0.67
			(B) SWNTs			
$R_{armchair}$	−0.25	−0.56	0.30	0.99	−0.58	0.32
R_{zigzag}	−0.56	−0.52	0.57	0.98	−0.25	0.53
			(C) 5/7 SWNTs			
$R_{armchair}$	−0.05	0.09	0.25	0.99	−0.35	0.11
R_{zigzag}	0.31	−0.30	0.41	0.98	−0.47	0.35

^{a} E_{bond}, E_{angle}, E_{dih}, E_{vdW}, $E_{str-bend}$, and E_{ele} are bond, bond angle, dihedral, van der Waals interaction, stretch−bend, and electrostatic energies, respectively.

barriers that prevent macrocycles from being released from C$_{60}$. These barriers keep C$_{60}$ encapsulated within the macrocycle ring.

Interestingly, the calculated energies before encapsulation and the energy after the macrocycle releases C$_{60}$ are different. The difference is a little bit larger for macrocycle **1**, which is the more stabilizing macrocycle by complexation. This suggests that the binding of macrocycles may change their geometries and energies. This is also observed with SWNTs, and is discussed below. The correlation coefficient (R) is a number between −1 and +1 that measures the degree to which two variables are linearly related. If there is a perfect linear relationship with a positive slope between the two variables, we have a correlation coefficient of 1. The correlation coefficients between the energetic variables and total energy are shown in Table 1. The correlations between the total energy and van der Waals (vdW) energy for both macrocycles **1** and **2** are significant ($R = 0.95$), while other energies show no strong correlations with total energy. This shows that the vdW energy is the key energetic term that accounts for the energetic stabilization of the C$_{60}$/macrocycle complex. Rotation of C$_{60}$ inside the macrocycle can also affect the energetic stability of the C$_{60}$/macrocycle complex. To examine this possibility, we monitored the energy changes while rotating (every 30°, from 0° to 180°) and minimizing C$_{60}$ with macrocycle **1** for their most stable complex structure. There are negligible fluctuations of energies (less than 0.9 kcal/mol), and therefore, there is no significant energetic change upon rotating C$_{60}$ inside the macrocycle.

SWNTs. In the proof-of-concept simulation, macrocycle **2** encapsulates armchair and zigzag SWNTs. As we can see from Figure 3, inorganic macrocycles slide along the SWNTs (moving the macrocycle every 1 Å along the z-axis of the nanotube), and energies for each point have been calculated. Energy profiles for all these calculations are shown in Figure 4. E_{encap} values

of armchair and zigzag SWNTs are −56.3 and −112.3 kcal/mol, respectively. The zigzag SWNT is much more stabilized by the inorganic macrocycle encapsulation. The calculation results and correlation coefficients of molecular mechanical energies and dipole moments with total energy are tabulated in Tables 1B and 2. Significantly, the energy is more stabilized when the macrocycle is located on the middle of the SWNT and there is an energetic barrier to overcome for the complete encapsulation of the SWNT with the macrocycle. Major energetic terms of both types of SWNTs for the energetic barrier formation are the dihedral and bond-stretch terms (E_{dih} and $E_{str-bend}$) of the macrocycle. Only those two terms clearly increase from off/before to on/maximum, while E_{vdW} still significantly decreases when compared with the off/before value (Table 2). If this energetic barrier is not overcome, the macrocycle will stay bound at the edge of the SWNT without further encapsulation. The overall energy profile suggests that the SWNT is ligated by the inorganic macrocycle. For both types of SWNTs, the energetic wells show stepwise optimization behaviors with energetic fluctuations (Figure 4A). E_{vdW} terms show significant correlation with total energy for both armchair and zigzag SWNTs. No other energetic terms show high correlations with total energy.

For armchair SWNTs, the off/before energy is lower than the off/after energy, but the off/after energy is rather more stable than the off/before energy in the case of zigzag SWNTs. This implies that there are permanent changes of molecular geometries engendered by the macrocycle encapsulation. To understand this behavior, macrocycle, SWNT, and interaction ($E_{ring/SWNT}$ − (E_{ring} + E_{SWNT})) energies are individually calculated in the case of armchair SWNTs. The correlation coefficient between interaction energies and total energies is 0.92. Energies of noninteracting SWNTs change from 1583.0 (off/before) to 1583.8 (on/minimum) kcal/mol, while energies of noninteracting macrocycles are changed from 1121.3 to 1150.9 kcal/mol. The interaction energy for off/before is −0.17 kcal/mol, while the interaction energy for on/minimum is −86.9 kcal/mol. This suggests that energetic stabilization is mainly from geometric optimization of the macrocycle and interaction between the SWNT and macrocycle. More calculations about this behavior are shown and discussed in a later section, RMS Deviations.

Monitoring the change of the dipole moments of the SWNTs provides us with structural and electronic insight into our systems. Dipole moments have been calculated, and total energies are shown in Figure 5. During encapsulation, there are large dipole moment changes (2.80−11.18 D for armchair SWNTs and 2.49−12.37 D for zigzag SWNTs). The dipole
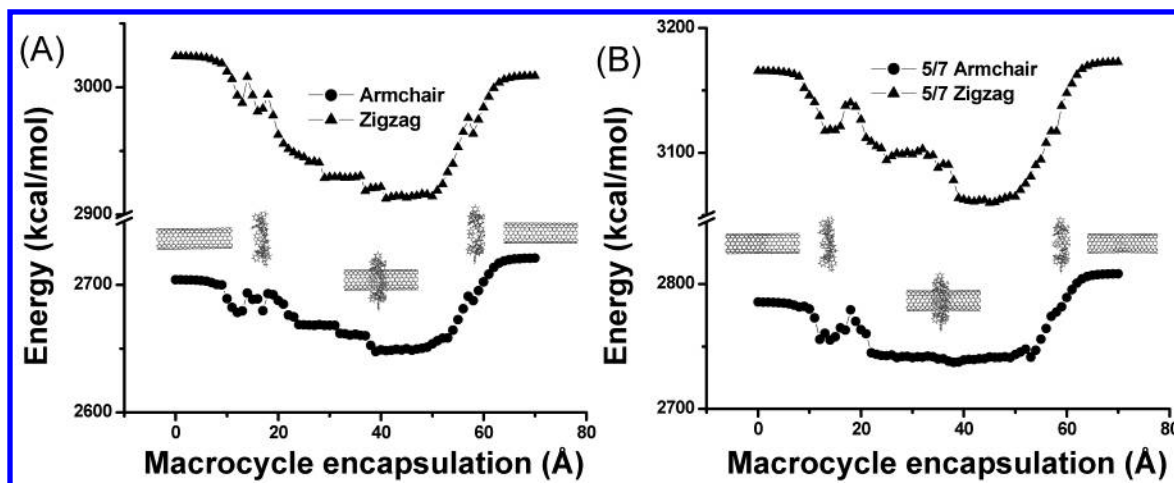
Figure 4. Energy profiles of macrocycle-encapsulated SWNTs. (A) Normal SWNTs. (B) SWNTs with pentagon−heptagon defects.

TABLE 2: Major Physical Values in the Process of Encapsulation[a]

	armchair SWNTs								zigzag SWNTs						
	E_{total}	E_{bond}	E_{angle}	E_{dih}	E_{vdW}	$E_{str-bend}$	E_{ele}	DP	E_{total}	E_{bond}	E_{angle}	E_{dih}	E_{vdW}	$E_{str-bend}$	E_{ele}	DP
off/before	2704.2	33.4	1223.2	1041.5	428.8	−28.4	5.6	3.5	3024.3	63.7	1169.3	1055.2	760.6	−30.1	5.6	3.5
on/maximum	2693.7	31.0	1221.4	1043.5	419.4	−27.6	5.9	2.8	3008.1	56.8	1167.6	1062.1	745.0	−29.2	5.8	2.5
on/minimum	2647.8	35.3	1231.8	1034.0	368.1	−26.9	5.5	10.7	2912.6	66.2	1172.5	1048.3	650.3	−30.2	5.5	11.5
off/after	2721.0	35.7	1227.3	1033.1	447.2	−27.7	5.5	11.2	3008.9	65.4	1152.1	1047.6	768.9	−30.6	5.5	11.9

	5/7 armchair SWNTs								5/7 zigzag SWNTs						
	E_{total}	E_{bond}	E_{angle}	E_{dih}	E_{vdW}	$E_{str-bend}$	E_{ele}	DP	E_{total}	E_{bond}	E_{angle}	E_{dih}	E_{vdW}	$E_{str-bend}$	E_{ele}	DP
off/before	2785.5	43.2	1276.5	1064.4	423.4	−27.5	5.6	3.5	3165.5	94.9	1252.4	1087.2	753.1	−27.8	5.6	3.5
on/maximum	2779.4	43.3	1283.1	1059.0	413.2	−24.9	5.6	8.1	3140.1	93.3	1264.3	1081.0	720.4	−24.5	5.7	7.3
on/minimum	2737.3	45.4	1284.0	1057.4	370.6	−25.6	5.5	10.1	3059.7	93.2	1251.2	1079.6	656.7	−26.4	5.5	11.1
off/after	2808.3	46.4	1281.6	1056.8	443.6	−25.8	5.5	10.5	3172.6	96.5	1248.0	1077.8	772.0	−27.3	5.5	11.7

[a] All energies are in kilocalories per mole, and the dipole moment (DP) is in debyes.
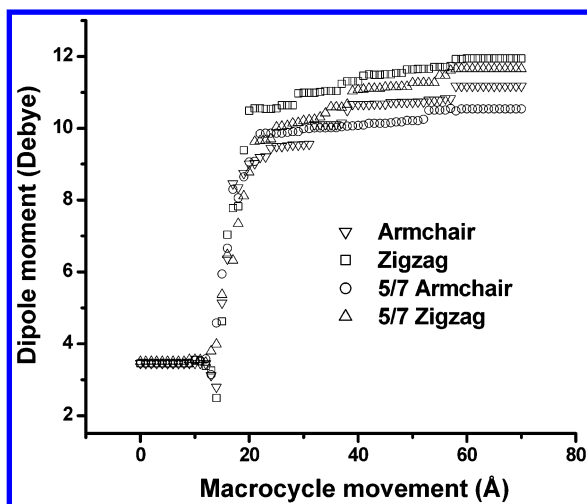

Figure 5. Dipole moment profiles of macrocycle-encapsulated SWNTs.

Figure 6. 5/7 defects (ball-and-stick) of armchair and zigzag SWNTs.

moment changes are similar for armchair and zigzag SWNTs. When macrocycles are located in the 10 and 20 Å region, there are large variations of both the dipole moments and energies of macrocycle/SWNT complexes (Figure 5). Notice that this region forms energetic barriers for both armchair and zigzag SWNTs and E_{encap} is larger for zigzag SWNTs. Overall, this obvious dipolar change upon binding of a macrocycle implies that this type of modification of an SWNT can alter electronic and structural properties of SWNT/macrocycle complexes (it is important to recall, however, that MM+ is not reliable for quantitative dipole moment calculation).
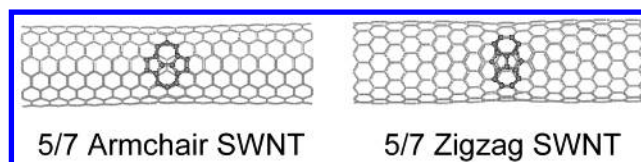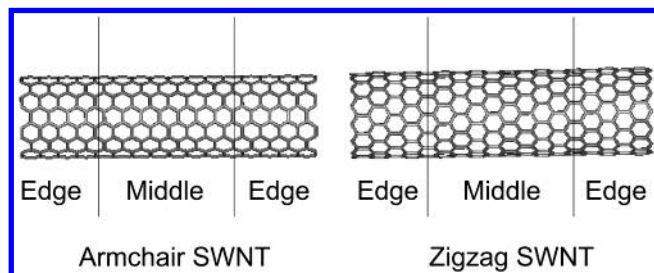
Pentagon−Heptagon Defects. Carbon nanotubes often contain defects, and topological defects such as the pentagon−heptagon (5/7) defect can create a local deformation in the width of the nanotube and significantly perturb the electronic properties of the hexagonal network of the nanotube.[27] Two pairs of pentagon−heptagon defects were introduced into the middle of both armchair and zigzag SWNTs (Figure 6), and E_{encap} for macrocycle **1** was calculated. E_{encap} values for 5/7 SWNTs are −48.0 kcal/mol (armchair) and −105.8 kcal/mol (zigzag). Again the zigzag SWNT is much more stabilized by macrocycle encapsulation than the armchair SWNT. E_{encap} values for 5/7 SWNTs are slightly smaller than those for normal SWNTs. The energy profile of a 5/7 armchair SWNT shows small stabilization with many fluctuations. Overall energetic behaviors for both armchair and zigzag SWNTs are similar to those of normal SWNTs. The energetic well area of a 5/7 armchair SWNT is smoother and wider than that of a normal armchair SWNT. E_{vdW} is the major contributing term for the total energy change of 5/7 SWNTs. There are entrance barriers for SWNT/macrocycle complexation (see Table 2). Dipolar changes for both 5/7 armchair and zigzag SWNTs are similar to those of normal SWNTs (Figure 5 and Table 2), but the magnitudes of dipolar changes are smaller than those of normal SWNTs.

SWNTs and C$_{60}$ Encapsulated by a Macrocycle

J. Phys. Chem. B, Vol. 107, No. 20, 2003 **4709**

TABLE 3: RMS Values (angstroms) for Superposed Armchair SWNTs and Macrocycles

	armchair		5/7 armchair		zigzag		5/7 zigzag	
	SWNT	ring[a]	SWNT	ring	SWNT	ring	SWNT	ring
			(A) Off/Before vs On/Minimum					
RMS$_{edge}$	0.025		0.031		0.045		0.119	
RMS$_{middle}$	0.044		0.037		0.049		0.072	
RMS$_{overall}$	0.035	2.247	0.035	2.105	0.047	2.646	0.121	2.668
			(B) Off/Before vs Off/After					
RMS$_{edge}$	0.029		0.029		0.022		0.103	
RMS$_{middle}$	0.024		0.022		0.021		0.069	
RMS$_{overall}$	0.027	2.377	0.028	2.236	0.022	2.822	0.112	2.820

[a] Large RMS values for macrocycles are due to the rotations of all four benzene rings and subsequent overall structural distortions within the macrocycle structures upon the binding onto SWNTs.

Figure 8. Structural changes between off/before (black line) and on/minimum (gray stick) for armchair SWNTs.

Figure 7. Division of SWNTs for RMS evaluation.

RMS Deviations. RMS deviation of Cartesian coordinates (x, y, z) is defined as the square root of the arithmetic average of a set of squared differences between two coordinate values. The RMS fit can give us insight into these asymmetric behaviors of energetic profiles. Two RMS fittings (off/before vs off/after and off/before vs on/minimum) have performed in this regard. To investigate the distortion of SWNTs by macrocycle encapsulation in greater detail, an SWNT is divided into three regions for both armchair and zigzag SWNTs (Figure 7 and Table 3) and two SWNTs are overlaid to minimize the RMS error of each region. In the case of RMS fittings of overlaid off/before and on/minimum SWNTs and macrocycles, RMS deviations are larger in the middle than at the edge of SWNTs due to stronger macrocycle/SWNT interaction in the middle part of SWNTs except 5/7 zigzag SWNTs (Table 3A). For 5/7 zigzag SWNTs, the RMS deviation is relatively larger than those of other types of SWNTs and the difference in RMS between the middle part and edge part of the SWNT is noticeable due to the 5/7 defect. Interestingly, RMS deviations are not large and almost the same as those of normal armchair SWNTs in the case of 5/7 armchair SWNTs, and this behavior also holds for RMS deviations between off/before and off/after. Most significantly, RMS deviations for macrocycles are much larger than those for SWNTs. This shows that the macrocycle is responsible for most of the structural adjustment of the SWNT/macrocycle complex. Figure 8 clearly shows that there is dramatic structural adjustment for the macrocycle (black line for off/before and gray stick for on/minimum) but there is nearly no change for the armchair SWNT during the encapsulation process. This behavior is the same for all four types of SWNTs.

For RMS fittings of overlaid off/before and off/after, RMS deviation values are smaller in the middle parts of SWNTs (Table 3B). The edges of SWNTs are affected slightly more by macrocycle encapsulation than the middle part. This off/before and off/after comparison is important to understand the computed discrepancies between total energy for off/before and total energy for off/aft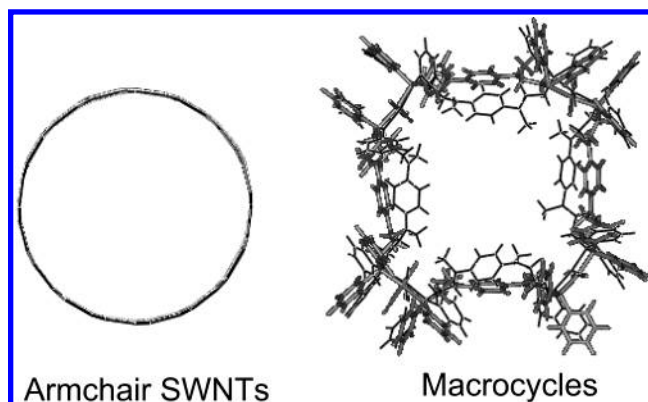er for all four SWNTs. As we can see from Table 3B, RMS deviations of macrocycles are much larger than those of SWNTs for all four types of SWNTs (see the footnote in Table 3). This indicates that total energy discrepancies between off/before and off/after for all SWNTs (Figure 4) are mostly due to the permanent structural change of the macrocycle.

Desolvation. Removing the water molecules around the nanotubes (desolvation) should be an important process for the binding of macrocycles onto SWNTs. An explicit water model has been used to examine the energetics for desolvation. To evaluate the desolvation energy, nanotubes are located in a water box (WB, with 2554 water molecules for both armchair and zigzag SWNTs). The total energies of the two configurations were compared. One configuration is before the macrocycle encapsulates the SWNT, and the other configuration is after encapsulation (the more stable configuration for the vacuum environment). Wetted encapsulation was evaluated:

$$\Delta E_{\text{wet encap}} = E_{\text{WB+ring+SWNT}}$$
(after engagement, minimized complex) $- E_{\text{WB+ring+SWNT}}$
(before engagement; the distance between the SWNT
and macrocycle is 10 Å closer than that for off/before)

It turns out that the encapsulation processes for both zigzag and armchair SWNTs are still energetically favored, and this means that macrocycle encapsulations for both armchair and zigzag SWNTs, even in a water environment, are plausible (Table 4). Encapsulation is more favorable for the zigzag SWNT ($\Delta E_{\text{wet encap}} = -36.4$ kcal/mol) than for the armchair SWNT ($\Delta E_{\text{wet encap}} = -26.6$ kcal/mol). Overall, there are large encapsulation stabilization energies for wetted encapsulation, and the macrocycle-encapsulated SWNT (for both armchair and zigzag) is still more favored than the separated macrocycle and SWNT. This implies that macrocycle encapsulation can help SWNTs dissolve in solvent. The major stabilization comes from E_{ele}, and there are also dipole moment changes (7 D for armchair and 22 D for zigzag SWNTs) from SWNT$_{\text{ring/off}}$ to SWNT$_{\text{ring/on}}$. Macrocycle encapsulation reduces the hydrophobic surface of the SWNT, and this helps the SWNT become soluble in water. The structural readjustment by solvation for armchair SWNTs may be a reason for the reduced difference in desolvation energies between armchair and zigzag SWNTs. This structural readjustment process costs more energy so that the more flexible armchair SWNT is less favored for the wetted encapsulation process.

TABLE 4: Desolvation Energies[a]

	E_{total}	E_{bond}	E_{angle}	E_{dih}	E_{vdW}	$E_{str-bend}$	E_{ele}	DP
armchair$_{off/before}$	−4254.73	34.20	1263.32	1042.85	−1865.06	−28.76	−4701.28	36.98
armchair$_{on/minimum}$	−4281.31	35.36	1279.82	1034.77	−1846.91	−26.61	−4757.74	43.73
stabilization	−26.58	1.16	16.50	−8.08	18.15	2.15	−56.46	6.75
zigzag$_{off/before}$	−4170.56	64.20	1216.48	1053.20	−1716.04	−30.05	−4758.36	36.49
zigzag$_{on/minimum}$	−4206.96	65.48	1210.73	1047.37	−1713.11	−30.97	−4786.47	58.51
stabilization	−36.40	1.28	−5.75	−5.83	2.93	−0.91	−28.11	22.02

[a] All energies are in kilocalories per mole, and dipole moment (DP) is in debyes.

Conclusions

Molecular mechanical energetics study of macrocycle-encapsulated C_{60} and SWNTs shows that the encapsulation processes with macrocycles are energetically probable, with several unique behaviors including different dipole moment changes for armchair and zigzag SWNTs. *The geometry is unconstrained, except for requiring 4-fold symmetry around Rh.* The van der Waals energy seems to be the main energetic term driving these encapsulation processes. During the encapsulation process, energetic barriers intervene before the complete encapsulation of SWNT occurs. A zigzag SWNT is more stabilized by encapsulation of macrocycles than an armchair SWNT. The defects on SWNTs influence the stability and energetic behavior of macrocycle-encapsulated SWNTs. The energetically stable well area is deeper for the 5/7 zigzag SWNT than for the normal zigzag SWNT. A permanent structural change has been observed after the macrocycle leaves the zigzag SWNT, while the energetic change is smaller after the macrocycle leaves the armchair SWNT. Upon the binding of the macrocycle, the dipole moment changes of zigzag and 5/7 zigzag SWNTs are more obvious than those of armchair and 5/7 armchair SWNTs. All these results agree with the argument of Lieber and co-workers[8] that the change of the environment of an SWNT can alter its physical properties. Energetic stabilization by macrocycle encapsulation is still large in a water environment, suggesting that wrapping an inorganic macrocycle around SWNTs can promote the solubility of SWNTs. Although we are able to exploit and explain the structures and energetics of C_{60}/macrocycle and SWNT/macrocycle complexes, the limitations of molecular mechanical calculations such as the inadequacy of the delocalization energy and the *nonreactive nature* should be noticed. Overall, this simulation demonstrates the possibility of tuning the physical properties of SWNTs and C_{60} by encapsulation within inorganic macrocycles and specific macrocycles with different functionality and size can capture specific SWNTs of various chiralities and sizes.

References and Notes

(1) Dresselhaus, M. S.; Dresselhaus, G.; Eklund, P. C. *Science of Fullerenes and Carbon Nanotubes*; Academic: San Diego, 1996.

(2) Hamada, N.; Sawada, S. I.; Oshiyama, A. *Phys. Rev. Lett.* **1992**, *68*, 1579.

(3) Wilder, J. W. G.; Venema, L. C.; Rinzler, A. G.; Smalley, R. E.; Dekker, C. *Nature* **1998**, *391*, 59.

(4) Bockrath, M.; Cobden, D. H.; Lu, J.; Rinzler, A. G.; Smalley, R. E.; Balents, L.; McEuen, P. L. *Nature* **1999**, *397*, 598.

(5) Dekker C. *Phys. Today* **1999**, *52*, 22.

(6) Andriotis A. N.; Menon M.; Srivastava D.; Froudakis G. *Phys. Rev. B* **2001**, *64*, 193401.

(7) Odom, T. W.; Huang, J.-L.; Kim, P.; Lieber, C. M. *Nature* **1998**, *391*, 62.

(8) Ouyang, M.; Huang, K.-L.; Cheung, C. L.; Lieber, C. M. *Science* **2001**, *292*, 702.

(9) Hu, J.; Odom, T. W.; Lieber, C. M. *Acc. Chem. Res.* **1999**, *32*, 435.

(10) Odom, T. W.; Huang, J.-L.; Kim, P.; Lieber, C. M. *J. Phys. Chem. B* **2000**, *104*, 2794.

(11) Hirsch, A. *Angew. Chem., Int. Ed.* **2002**, *41*, 1853.

(12) Steuerman, D. W.; Star, A.; Narizzano, R.; Choi, H.; Ries, R.; Nicolini, C.; Stoddart, J. F.; Heath, J. R. *J. Phys. Chem. B* **2002**, *106*, 3124.

(13) Frankland S. J. V.; Caglar A.; Brenner D. W.**;** Griebel M. *J. Phys. Chem. B* **2002**, *106*, 3046.

(14) O'Connell, M. J.; Boul, P.; Ericson, L. M.; Hauffman, C.; Wang, Y.; Haroz, E.; Kuper, C.; Tour, J.; Ausman, K. D.; Smalley, R. E. *Chem. Phys. Lett.* **2001**, *342*, 265.

(15) Smith, B. W.; Monthioux, M.; Luzzi, D. E. *Nature* **1998**, *396*, 323.

(16) Okada, S.; Saito, S.; Oshiyama, A. *Phys. Rev. Lett.* **2001**, *86*, 3835.

(17) Hornbaker, D. J.; Kahng, S.-J.; Misra, S.; Smith, B. W.; Johnson, A. T.; Mele, E. J.; Luzzi, D. E.; Yazdani, A. *Science* **2002**, *295*, 828.

(18) Liu, X.; Stern, C. L.; Mirkin, C. A. *Organometallics* **2002**, *21*, 1017.

(19) Balch, A. L.; Catalano, V. J.; Lee, J. W. *Inorg. Chem.* **1991**, *30*, 3980.

(20) Balch, A. L.; Catalano, V. J.; Lee, J. W.; Noll, B. C.; Olmstead, M. M. *Inorg. Chem.* **1993**, *32*, 3577.

(21) Bashilov, V. V.; Petrovskii, P. V.; Sokolov, V. I.; Lindeman, S. V.; Guzey, I. A.; Struchkov, Y. T. *Organometallics* **1993**, *12*, 991.

(22) Green, M. L. H.; Stephens, A. H. H. *Chem. Commun.* **1997**, 793.

(23) Allinger, N. L. *J. Am. Chem. Soc.* **1977**, *99*, 8127.

(24) Burkert, U.; Allinger, N. L. *Molecular Mechanics*; ACS Monograph 177; American Chemical Society: Washington, DC, 1982.

(25) Lii, J.-H.; Gallion, S.; Bender, C.; Wikström, H.; Allinger, N. L.; Flurchick, K. M.; Teeter, M. M. *J. Comput. Chem.* **1989**, *10*, 503.

(26) Jorgensen, W. L.; Chandrasekhas, J.; Mandura, J. D.; Impey, R. W.; Klein, M. L. *J. Chem. Phys.* **1983**, *79*, 926.

(27) Charlier, J.-C.; Ebbesen, T. W.; Lambin, P. *Phys. Rev. B* **1996**, *53*, 11108.